Article

Not peer-reviewed version

Influence of Sonication on the Molecular Characteristics of Carbopol® and Its Rheological Behavior in Aqueous Dispersions and Microgels

José Pérez-González *, Yusef Muñoz-Castro, Francisco Rodríguez-González, Benjamín M. Marín-Santibáñez, Esteban F. Medina-Bañuelos

Posted Date: 5 June 2024

doi: 10.20944/preprints202406.0259.v1

Keywords: Carbopol® Ultrez 10 microgels; rheology; yield-stress fluids; ultrasonication; Fourier transform infrared (FTIR) spectroscopy; confocal microscopy

 doi:10.20944/preprints202406.0259.v1

Article

Influence of Sonication on the Molecular Characteristics of Carbopol® and Its Rheological Behavior in Aqueous Dispersions and Microgels

José Pérez-González [1,*], Yusef Muñoz-Castro [1], Francisco Rodríguez-González [2], Benjamín M. Marín-Santibáñez [3] and Esteban F. Medina-Bañuelos [3]

[1] Laboratorio de Reología y Física de la Materia Blanda, Escuela Superior de Física y Matemáticas, Instituto Politécnico Nacional, U. P. Adolfo López Mateos, C. P. 07738 Ciudad de México, México; yusefmunoz@gmail.com

[2] Departamento de Biotecnología, Centro de Desarrollo de Productos Bióticos, Instituto Politécnico Nacional, Carretera Yautepec-Jojutla Km. 6, Calle CEPROBI No. 8, Col. San Isidro, Yautepec, C. P. 62731, Morelos, México; frrodriguezg@ipn.mx

[3] Escuela Superior de Ingeniería Química e Industrias Extractivas, Instituto Politécnico Nacional, U. P. Adolfo López Mateos, C. P. 07738 Ciudad de México, México; bmarin@.ipn.mx, efmedinab1400@alumno.ipn.mx

* Correspondence: jperezgo@ipn.mx

Abstract: The effect of sonication on the molecular characteristics of poliacrylic acid (Carbopol® Ultrez 10) and its rheological behavior in aqueous dispersions and microgels containing 0.25 wt. % of the polymer was analyzed in this work by rheometry, weight-average molecular weight (M_w) measurements via static light scattering (SLS), Fourier transform infrared (FTIR) spectroscopy and confocal microscopy. For this, the precursor dispersion and the microgels were sonicated in a commercial ultrasound bath at constant power and different times. We observed a softening of the microgel microstructure consisting of a systematic decrease in its shear modulus, yield stress and viscosity with increasing sonication time, while their overall Herschel-Bulkley (H-B) behavior was preserved. SLS measurements evidenced a reduction of M_w of polyacrylic acid with sonication time. Separately, FTIR measurements indicate that sonication produces scission in the C-C links of the Carbopol® backbone, which results in chains with the same chemistry but lower molecular weight. Finally, confocal microscopy measurements revealed a concomitant diminution of the size of the microsponge domains with sonication time, which is reflected in a softer microstructure resulting from reduction of the molecular weight of polyacrylic acid. The present results indicate that both the microstructure and the rheological behavior of Carbopol® microgels, in particular, and complex fluids in general, may be manipulated or tailored by high-power ultrasonication.

Keywords: Carbopol® Ultrez 10 microgels; rheology; yield-stress fluids; ultrasonication; Fourier transform infrared (FTIR) spectroscopy; confocal microscopy

1. Introduction

Sonication or ultrasonication is the application of ultrasound energy to a sample, which most often consists of a fluid with dispersed particles. There are two main ways for sonication, namely, by using an ultrasonic bath or a probe sonicator. In the first mode, the fluid in a vessel is set in a water-containing ultrasonic bath; in the second, the ultrasonic probe is directly immersed into the fluid of interest. Applications of ultrasound may be roughly divided into low-power (<1 W/cm^2) and high-frequency (>100 kHz) regime, as well as in high-power (>1 W/cm^2) and low-frequency (20–100 kHz) regime, being the first mainly used for non-destructive analysis or materials characterization, while the second is used in industrial processes as well as to produce chemical reactions and changes in the microstructure of materials [1,2].

 doi:10.20944/preprints202406.0259.v1

According to the Royal Society of Chemistry [3], propagation of ultrasonic waves (typically >20 kHz) in a liquid medium results in agitation along with alternating high-pressure (compression) and low-pressure (rarefaction) cycles. During rarefaction, high-intensity sonic waves create small vacuum bubbles or voids in the liquid, which then collapse violently (cavitation) during compression, creating very high local temperatures. Thus, prolonged high-intensity sonication may produce chemical reactions in a sample. This fact, which was known since the early decades of the last century, resulted in the establishment of sonochemistry as a field, after the first international symposium on sonochemistry organized by the Royal Society of Chemistry in 1986 and the influencing reviews by Lorimer and Mason [1] and Lindley and Mason [2], respectively. Afterward, high-intensity sonication has been exploited in many applications, including ultrasonic cleaning, drilling, soldering, chemical processes, emulsification, deagglomeration, extraction, cell disruption [4], and many others as those found in food science and processing [5–7].

An application of sonication of particular interest to this work is the possible manipulation or tailoring of the microstructure of complex fluids, including gels. Gels appear in many everyday products such as cosmetics, pharmaceuticals, detergents, coatings, and foods, among many others. Then, tuning the flow or rheological properties of gels using ultrasound may be of practical relevance. Interestingly, scarce work has been done to understand the gel structural changes and its concomitant rheological behavior arising from sonication. In this regard, Seshadri et al. [8] studied the effect of high-intensity ultrasound (40 W) at various times on the rheological and optical properties of high-methoxyl pectin (HMP) dispersions. These authors found that ultrasonically pretreated pectin dispersions formed weaker gels with increasing sonication power and time and resulted in more transparent gels. The results were attributed to an overall reduction in the average molecular weight of pectin due to cavitational effects. Zheng et al. [9] also analyzed the effects of sonication at different powers (120, 240, 360, and 480 W) on the rheological properties of HMP dispersions and showed that their viscosity was reduced significantly with increasing sonication power and time; meanwhile, the overall pseudoplastic behavior of the gel, was retained. Zheng et al. [9] suggested that the cavitation effect damaged the structure of HMP as ultrasonic power increased, leading to a significantly decreased strength of the gel.

Recently, Gibaud et al. [10] introduced what they called “rheoacoustic” gels, that is, colloidal gels sensitive to ultrasonic vibrations. These authors used a combination of rheological and structural characterization to evidence and quantify a strong softening, including decreased yield stress and accelerated shear-induced fluidization, in three different colloidal gels submitted to ultrasonic vibrations (with submicron amplitude and frequencies in the range between 20–500 kHz). The softening was attributed to micron-sized cracks within the gel network, which could or could not fully heal, depending on the acoustic intensity, once vibrations are turned off.

In this work, the effects of sonication time at a fixed power on the molecular characteristics of Ultrez 10 and its rheological behavior in a 0.25 wt. % dispersion in bi-distilled water and the resulting microgel after neutralization, were analyzed by rheometry, molecular weight measurements via static light scattering (SLS), Fourier transform infrared (FTIR) spectroscopy and confocal microscopy. For this, the precursor dispersion and the microgel were sonicated in a commercial ultrasound bath at constant power for different times. We observed a softening of the microgel microstructure consisting of a systematic decrease in its shear modulus, yield stress, and viscosity with increasing sonication time, while the Herschel-Bulkley behavior was maintained. SLS measurements evidenced a reduction of M_w of polyacrylic acid with sonication time. Separately, FTIR measurements indicate that sonication produces scission in the C-C links of the Ultrez 10 backbone, which results in chains with the same chemistry but lower molecular weight. Finally, confocal microscopic measurements revealed a concomitant diminution of the size of the microsponge domains, resulting from reduction of the molecular weight of polyacrylic acid with sonication time. Overall, results in this work indicate that both the microstructure and rheological behavior of microgels, in particular, and complex fluids in general, may be manipulated or tailored by high-power ultrasonication.

 doi:10.20944/preprints202406.0259.v1

2. Results and Discussion

2.1. Rheological Behavior of Non-Sonicated and Sonicated Microgels

To assess the changes in rheological behavior of the Ultrez 10 microgels due to ultrasound treatment, we performed oscillatory shear and rotational steady shear measurements. We first discuss the viscoelastic response in small amplitude oscillatory shear (SAOS) measurements, and afterward the steady shear behavior of the microgels.

2.1.1. Small Amplitude Oscillatory Shear Measurements

Figure 1(a) shows the absolute value of the complex shear modulus ($|G^*|$) measured in stress amplitude sweeps at an angular frequency (ω) of *6.28 rad/s* for the non-sonicated, SM0, and sonicated microgels samples, namely, SM60, SM120 and SM180 (the number in the labels represents the sonication time in minutes). Clearly, $|G^*|$ decreases with increasing the sonication time; its value in the linear viscoelastic region (LVR) decreases ~25%, from about 192 Pa for SM0 up to 159 Pa for SM180, evidencing a weakening or softening of the microgel microstructure due to the imposed ultrasound irradiation. Figure 1(b) indicates that the softening of the microgel microstructure can be mainly attributed to a decrease in its elastic response or elastic modulus (G') since the loss modulus (G'') barely changes in the LVR with increasing the sonication time. In addition, the limit of the LVR and the crossover point between G' and G'' decrease with increasing sonication time, which indicates that ultrasound treatment promotes anticipated fluidization. At last, Figure 1(c) shows the frequency swept for the microgel with different sonication times. Note that the G'/G'' ratios for different sonication times are almost *O(10)* or higher in the range of frequency analyzed, indicating that the 0.25 wt. % Ultrez 10 microgel remains as a strong gel [11] for the periods of irradiation in this work.

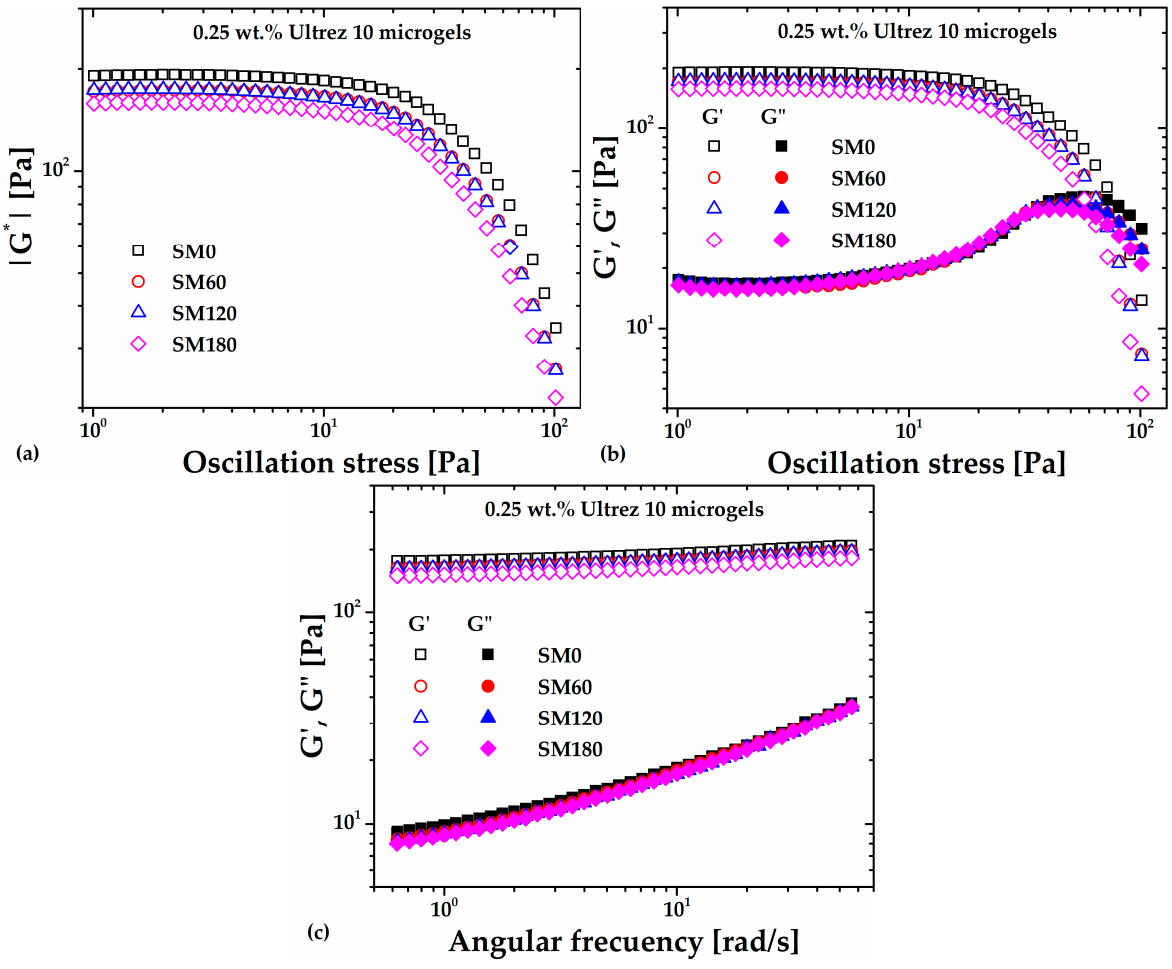

 doi:10.20944/preprints202406.0259.v1

Figure 1. SAOS measurements of the Ultrez 10 microgel submitted to different sonication times, (a) $|G^*|$ as a function of the oscillating stress; (b) G' and G'' as functions of the oscillating stress; at *6.28 rad/s*. (c) G' and G'' as functions of the angular frequency at 3 Pa.

2.1.2. Steady Shear Measurements

The flow curves of the microgel for different sonication times obtained under steady shear measurements are shown in Figure 2, which includes the flow curves for SM0 and SM180 obtained in up and down shear stress cycles. First, it can be seen that SM0 and SM180 up and down flow curves superpose very well, respectively, indicating that the microgel is originally non-thixotropic [12,13] and that sonication does not induce thixotropy. The same behavior was observed for all up and down flow curves (these are not included in Figure 2 so as not to make the plot heavy). Also, as the share rate tends to zero, all flow curves extrapolate to a critical shear stress value, i.e., the yield stress of the microgels. Irrespective of the sonication time, they are all very well described by the H-B constitutive model, $\sigma = \sigma_y + m\dot{\gamma}^n$, where σ is the shear stress, σ_y is the yield stress, m is the consistency index, $\dot{\gamma}$ is the shear rate, and n is the shear rate sensitivity index, in agreement with previous reports for similar non-sonicated microgels [12–17]. The H-B parameters for the microgels with different sonication times are shown in Table 1.

Table 1. Herschel-Bulkley parameters of 0.25 wt.% Ultrez 10 microgels sonicated at different times.

Microgels	σ_y [Pa]	m [Pa·s^n]	n [1]
SM0	37.2	19.2	0.37
SM60	31.6	16.0	0.38
SM120	26.4	14.0	0.37
SM180	19.6	12.6	0.39
SMD180	20.5	11.7	0.40

Significant decrease is observed, however, in the consistency index and yield stress of the microgel, that is, the first in an exponential way and the second linearly with increasing sonication time (Figure 3(a)). Regarding the power-law or shear thinning index of the microgel, this seems to remain constant, with a more significant variation for SM180. This anomalous behavior is evidenced in Figure 3(b), where the different flow curves have been superposed by plotting σ/σ_y as a function of the shear rate, see references [11,14,16]. Note that the SM180 flow curve departs from the superposed ones, indicating a dramatic change in the gel microstructure at long sonication times. Gutowski *et al*. [15] have interpreted different scaling among low- and high-concentration Ultrez 10 microgels as a signal of a significant change in the mesostructure of the materials, which agrees with the result in this work (see discussion in section 2.4 below).

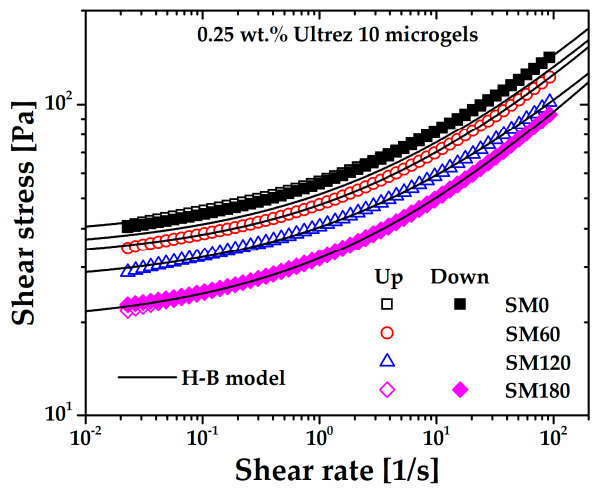

 doi:10.20944/preprints202406.0259.v1

Figure 2. Steady shear flow curves of the Ultrez 10 microgel for different sonication times. The flow curves for SM0 and SM180 obtained in up and down shear stress cycles are included as a proof of the absence of thixotropy.

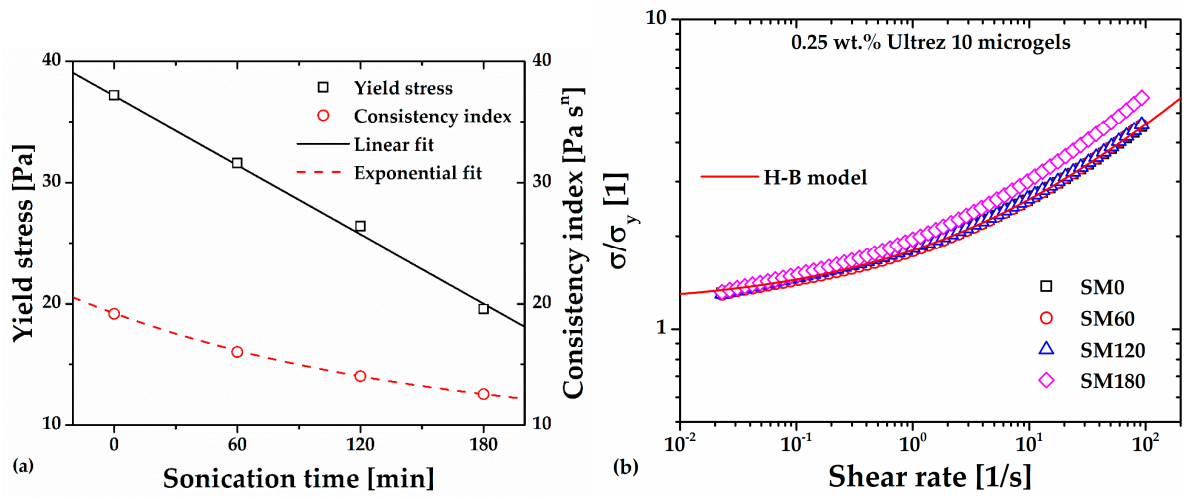

Figure 3. (a) Consistency index and yield stress of Ultrez 10 microgel as functions of sonication time. (b) σ/σ_y as a function of the shear rate.

The softening of the microgel microstructure and its approximately constant pseudoplastic behavior upon submission to sonication is consistent with previous reports for other gel systems [9,10]. From X-ray scattering measurements in their colloidal gels during sonication, Gibaud *et al*. [10] attributed this softening to micron-sized cracks within the gel network; these authors concluded that the gel network is fractured by ultrasonic vibrations and suggested that a more complete picture of the gel microstructure remained to be obtained. In sections 2.3-2.4, we provide such a picture on the basis of measurements of changes in the molecular characteristics of Ultrez 10 after sonication and confocal microscopy.

2.2. Rheometry of the Sonicated Ultrez 10 Dispersion and Its Microgel

In a different experiment to assess ultrasound irradiation induced damage of the molecular structure of polyacrylic acid, we sonicated a 0.25 wt.% Ultrez 10 dispersion for *180 min* (SD180) before proceeding to neutralization to form the microgel (SDM180). Figure 4 displays the steady-state flow curve of such dispersion before and after sonication. Both flow curves exhibit a slight non-Newtonian behavior characterized by power-law relationships ($\sigma = m\dot{\gamma}^n$ where σ is the shear stress, m is the consistency index, $\dot{\gamma}$ is the shear rate, and n is the shear rate sensitivity index). It can be observed that SD180 is a little less viscous than the non-sonicated one (SD0), as expected on the basis of possible ultrasound damage on the Ultrez 10 macromolecules, which would result in a decrease on its weight average molecular weight, M_w (see discussion below). Concomitantly, a softening effect of the microgel microstructure is expected. Measurements of the pH at the same temperature in the dispersion before and after sonication were 2.40±0.03, which indicates that ultrasound treatment does not influence the amount of ionized carboxyl groups in the dispersion.

 doi:10.20944/preprints202406.0259.v1

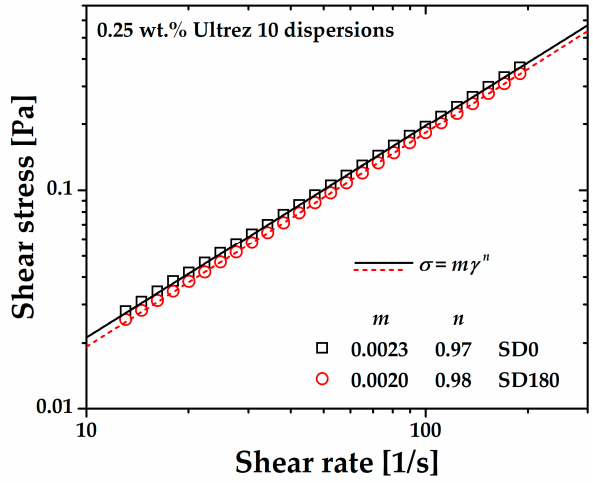

Figure 4. Steady state flow curves of the non-sonicated (SD0) and sonicated (SD180) 0.25 wt.% Ultrez 10 dispersions.

Figure 5a,b show the stress amplitude swept at an angular frequency (ω) of *6.28 rad/s* and the frequency swept at 3 Pa, respectively, for the microgel (SDM180) obtained from the SD180 dispersion (the sweeps corresponding to the SM0 and SM180 microgels are included for comparison). A slight decrease in the *G'* value is apparent for SDM180 in comparison with the SM180 sample, while the *G"* value does not change. Should ultrasound irradiation be breaking polyacrylic acid macromolecules, the small decrease in G' could be attributed to the formation of the SDM180 microgel from shorter molecules, i. e., with reduced molecular weight, leading to a slightly softer microgel structure than the SM180 microgel, which was composed from raw Ultrez 10. This result would agree with reports suggesting that stronger hydrogels are formed by increasing the degree of crosslinking (see Figure 6 in [18]) and/or the molecular weight of the polymer [19].

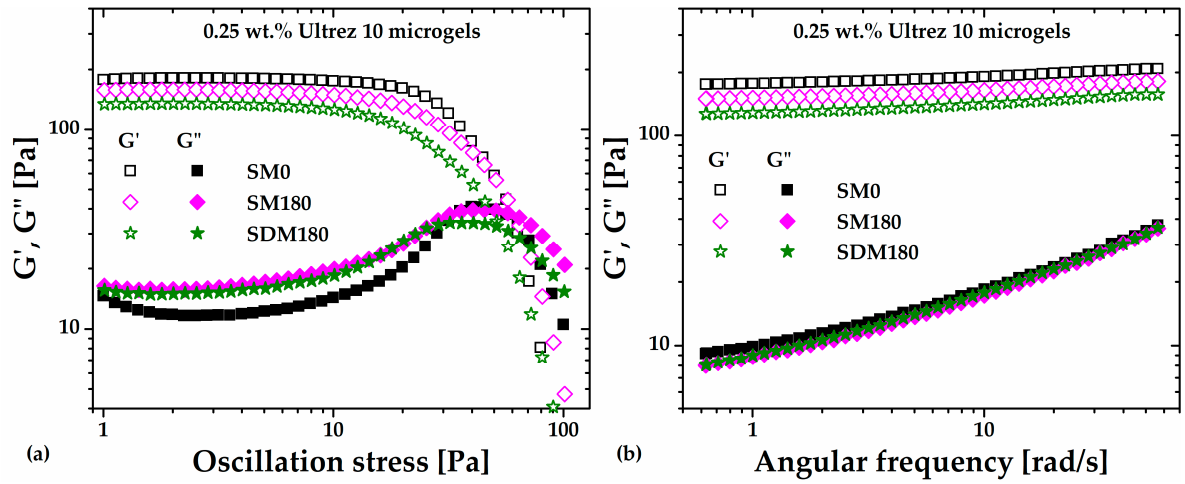

Figure 5. (a) Stress amplitude swept at *6.28 rad/s* and (b) frequency swept at 3 Pa for the Ultrez 10 microgel obtained from the sonicated precursor dispersion (SDM180). The sweeps corresponding to the SM0 and SM180 microgels are included for comparison.

2.3. Molecular Weight Measurements and FTIR of Ultrez 10 before and after Sonication

Molecules dissolved in water can undergo pyrolysis and free radical attack when submitted to sonication [4,20]. Also, macromolecules may be broken in their main chain due to sonication [20]. Different authors have reported the degradation of polymer molecules when submitted to sonication. For example, Schittenhelm and Kulicke [21] used ultrasonic degradation to create homologous series of molar masses for establishing structure-property relationships in cellulose derivatives. These authors reported a diminution of molecular mass and polydispersity for hydroxyethylsulfoethyl

 doi:10.20944/preprints202406.0259.v1

cellulose with increasing the sonication time. More recently, Zhong *et al*. [22] reported a decrease of the average molecular weight of schizophyllan, and degradation products with a narrower molecular weight distribution after ultrasonic treatment. Also, the original non-Newtoninan shear thinning behavior of untreated schizophyllan changed to a Newtonian one for the resulting fractions. To investigate the effect of ultrasound on the molecular structure of Ultrez 10 and its effect on microgel formation in this work, weight-average molecular weight (M_w) measurements using static light scattering (SLS) and Fourier transform infrared spectroscopy (FTIR) were performed on the raw and sonicated polymer as shown below.

To determine the M_w by SLS the refractive index, n, of Ultrez 10 dispersions was measured as a function of its concentration, c, the results are presented in Table 2 and plotted in Figure 6(a), respectively, for the SD0 and SD180 dispersions. The dn/dc values for each sample were obtained by linear fitting of the data, and the resulting equations are embedded in the Figure. These values were used to calculate the optical constant, K, which is necessary to obtain the Kc/R_θ values, presented also in Table 2 and plotted in Figure 6(b) *versus* c. The Rayleigh's ratios, R_θ, were calculated using the refractive indexes of water and toluene as well as the Rayleigh's ratio of toluene.

Table 2. Concentration of Ultrez 10 dispersions (c), n, and Kc/R_θ for M_w determination.

Sample	c [mg/mL]	0.00	0.25	0.50	0.75	1.00	1.50	2.00
SD0	n [1]	1.332485	1.332651	1.332753	1.332858	1.332983	1.333245	1.333540
	Kc/R_θ [mol/g]	--	--	4.4712E-6	4.703E-6	5.35064E-6	6.26993E-6	7.44143E-6
SD180	n [1]	1.332485	1.332605	1.332699	1.332845	1.332961	1.333205	1.333480
	Kc/R_θ [mol/g]	--	--	8.6022E-6	8.5915E-6	8.41236E-6	7.67077E-6	7.44605E-6

Measurements of n and Kc/R_θ were obtained at 25 ºC by using a refractometer and SLS technique (Litesizer™ 500).

In Figure 6(b), the dotted lines indicate the fittings to the Debye equation for SD0 and SD180. M_w and A_2 were calculated from the ordinate to the origin and the slope of each linear relationship for SD0 and SD180 samples, respectively, the resulting values are reported in Table 3. Clearly, the lowest M_w corresponds to the SD180 sample, which is less than half the value corresponding to SD0; this reflects the effect of ultrasound treatment on the molecular structure of Ultrez 10. Interestingly, A_2 changes from positive for SD0 to negative for SD180, indicating that polymer-solvent interactions are favored before sonication, meanwhile, polymer-polymer interactions are boosted after sonication [23].

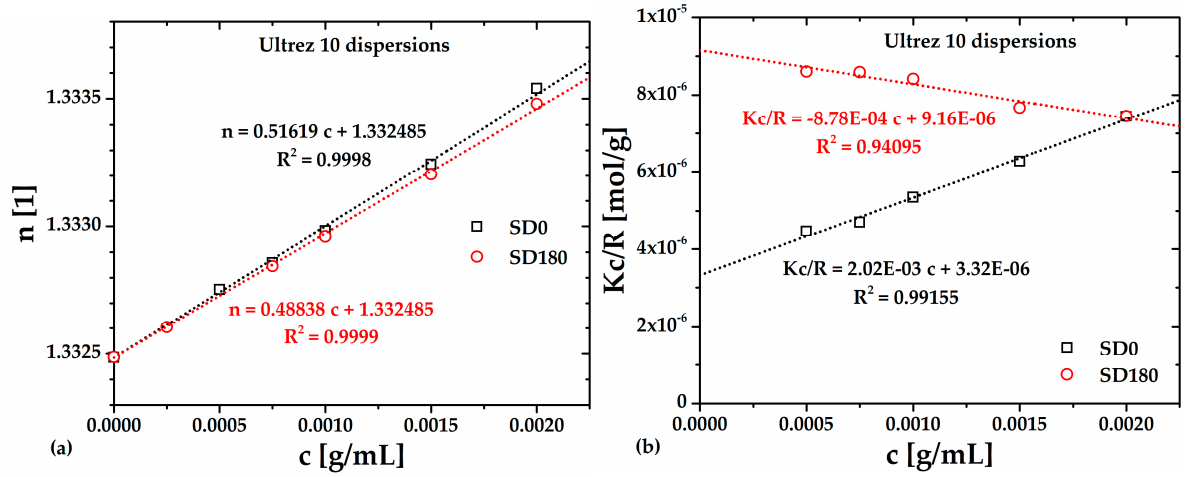

Figure 6. (a) n and (b) Kc/R_θ as functions of Ultrez 10 concentration.

 doi:10.20944/preprints202406.0259.v1

Table 3. M_w and A_2 of the Ultrez 10 before and after 180 minutes of sonication.

SD0		SD180	
M_w [mol/g]	A_2 [mol·cm³/g²]	M_w [mol/g]	A_2 [mol·cm³/g²]
300860.46	1.0102E-3	109212.04	-4.3999E-4

The data on this Table were obtained at 25 ºC by using a refractometer and SLS technique (Litesizer™ 500).

The change of sign in A_2 for the sonicated polymer (Figure 6(b)) has also been related to a change in the chemical structure of the macromolecule due to depolymerization induced by prolonged periods of sonication [24–30]. Figure 7 shows the Fourier transform infrared (FTIR) spectra of the lyophilized Ultrez 10 obtained from the SD0 and SD180 dispersions, respectively. For both samples, the peaks centered around 1705 and 1240 cm^{-1} corresponding to the stretching of C=O and C-O bonds, respectively, along with the broad band from 3700-2400 cm^{-1}, indicate the presence of carboxylic groups. In particular, the small band in between 2700-2400 cm^{-1} indicates dimer formation (overtone) or hydrogen bonding, which is characteristic of the polyacrylic acid in its solid (powder) state. In addition, the peaks located at low wavenumbers (<1000 cm^{-1}) can be attributed to the wagging of C-H that indicates the presence of C=C. Thus, the increase in height of these peaks for SD180 suggests scission of the C-C links in the backbone and the concomitant formation of C=C bonds at the ends of the new shorter and less polar polymer chains, which is consistent with the reduction of the molecular weight of Ultrez 10 and the change in sign of A_2. These results are consistent with previous reports on the effect of sonication on the molecular structure of other water-soluble polymers [22,27,30]. In addition, the reduction of the M_w of the Ultrez 10 in the aqueous solutions and microgels as well as their change in the rheological properties agree well with that induced by ultrasound treatment for schizophyllan [22], water-soluble polymers [27] and sodium alginate [30].

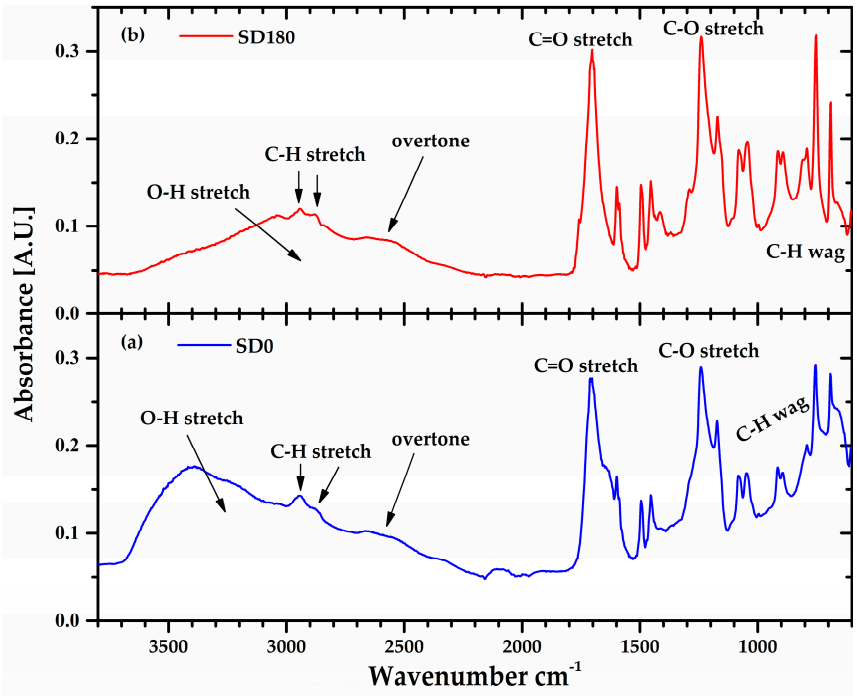

Figure 7. FTIR spectra of the lyophilized Ultrez 10 from the (a) non-sonicated (SD0) and (b) sonicated (SD180) precursor dispersions.

On the other hand, Figure 8 shows the FTIR spectra of the sonicated (SD180) and non-sonicated (SD0) aqueous dispersions, which appear remarkably well superimposed. The broad band from 3700 to 2900 cm^{-1} along with the peak centered at 1700 cm^{-1} attributed to O-H and C=O stretchings, respectively, are characteristic of carboxylic acid groups present along the backbone of polyacrylic acid. More importantly, the lack of a band for both SD0 and SD180 samples from 2800 to 2500 cm^{-1}, typical of carboxylic acids in their solid and liquid state, is indicative of complete dissociation of the

Preprints.org (www.preprints.org) | NOT PEER-REVIEWED | Posted: 5 June 2024 doi:10.20944/preprints202406.0259.v1

carboxylic acid groups [27], which is consistent with the pH=2.40±0.03 measured for both the SD0 and SD180 samples. Thus, this result suggests that the softening of the microgel may be attributed only to a decrease in the molecular weight of Ultrez 10 macromolecules due to depolymerization occurring in their main backbone [20].

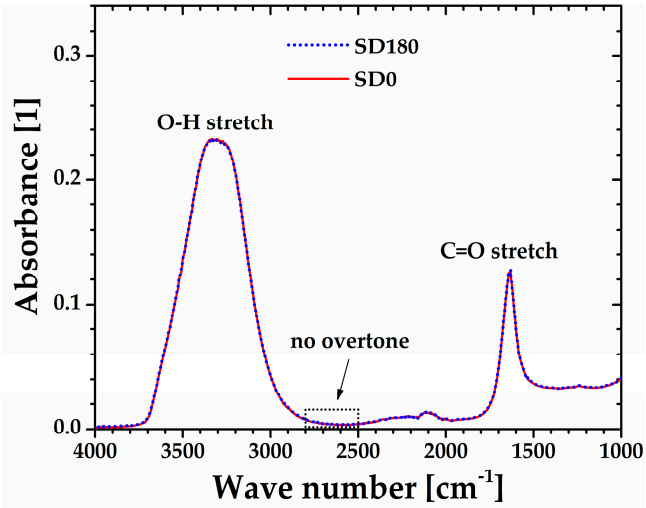

Figure 8. FTIR spectra of the non-sonicated (SD0) and sonicated (SD180) precursor dispersions.

A separate test of similarity between SM180 and SDM180 microgels is obtained from steady state flow measurements. Figure 9 shows the up and down flow curves of the SDM180 microgel as compared to SM0 and SM180 ones. First note that the SDM180 and SM180 exhibit almost the same flow behavior, i.e., they are very well described by the same H-B model. Then, the up and down SDM180 flow curves superimpose with the corresponding for SM180, indicating that ultrasound treatment before gel formation does not induce thixotropy either. Interestingly, this is consistent with the viscous response obtained from the oscillatory measurements in Figure 5, where the G" values are approximately the same for the SM180 and SDM180 microgels. Thus, these results further demonstrate that sonication of the precursor dispersion or the already formed gel produces softer microgels with similar shear rheological properties.

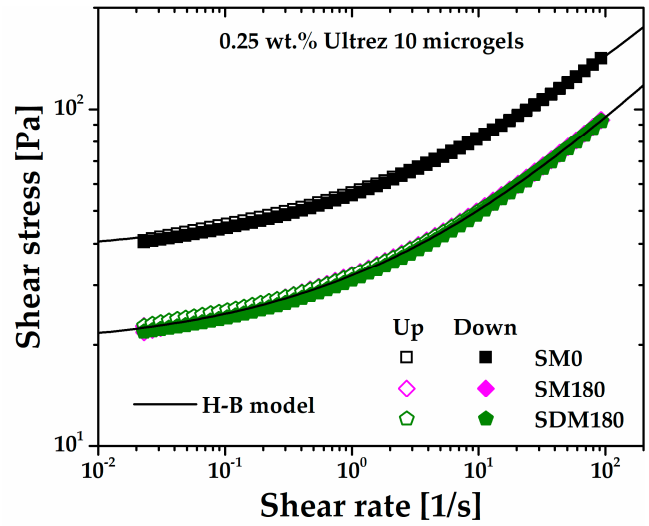

Figure 9. Up and down flow curves of the microgel SDM180. The flow curves corresponding for the SM0 and SM180 microgels are included for comparison.

 doi:10.20944/preprints202406.0259.v1

2.4. Confocal Microscopy of Non-Sonicated and Sonicated Ultrez 10 Microgels

Confocal microscopy observations of the non-sonicated and sonicated Ultrez 10 microgels were performed to evidence changes in their microstructure due to sonication. Figure 10a–e show the resulting characteristic microstructure of SM0, SM60, SM120, SM180 and SDM180 microgels, respectively. It can be observed that microgel microstructure becomes more open or less compact with increasing the sonication time, as well as for the SDM180 sample. The domains [31] appear to increase in size with sonication time leaving a less compact or more porous structure with more free solvent. Interestingly, the structure of the microgels with longer sonication time resembles that of less concentrated microgels (see for example [15,32]). Oelschlaeger *et al*. [32] analyzed the microstructure of Ultrez 10 microgels and its relationship with macroelasticity. These authors found that the bulk shear modulus, $|G^*|$, strongly depends on the fraction of compact regions formed by aggregated particles, in which less free solvent is available (see Figure 3 in [32]). It is expected that decreasing of such compact regions and more free solvent with increasing the sonication time results in enhanced lubrication among sponges and the concomitant decrease in viscoelastic characteristics of the microgel, these represented by the shear modulus, viscosity and yield stress, in agreement with results in Figures 1–3. Also, the SLS measurements presented above corroborate the change in molecular weight of Ultrez 10 macromolecules due to sonication, which results in softer microgels.

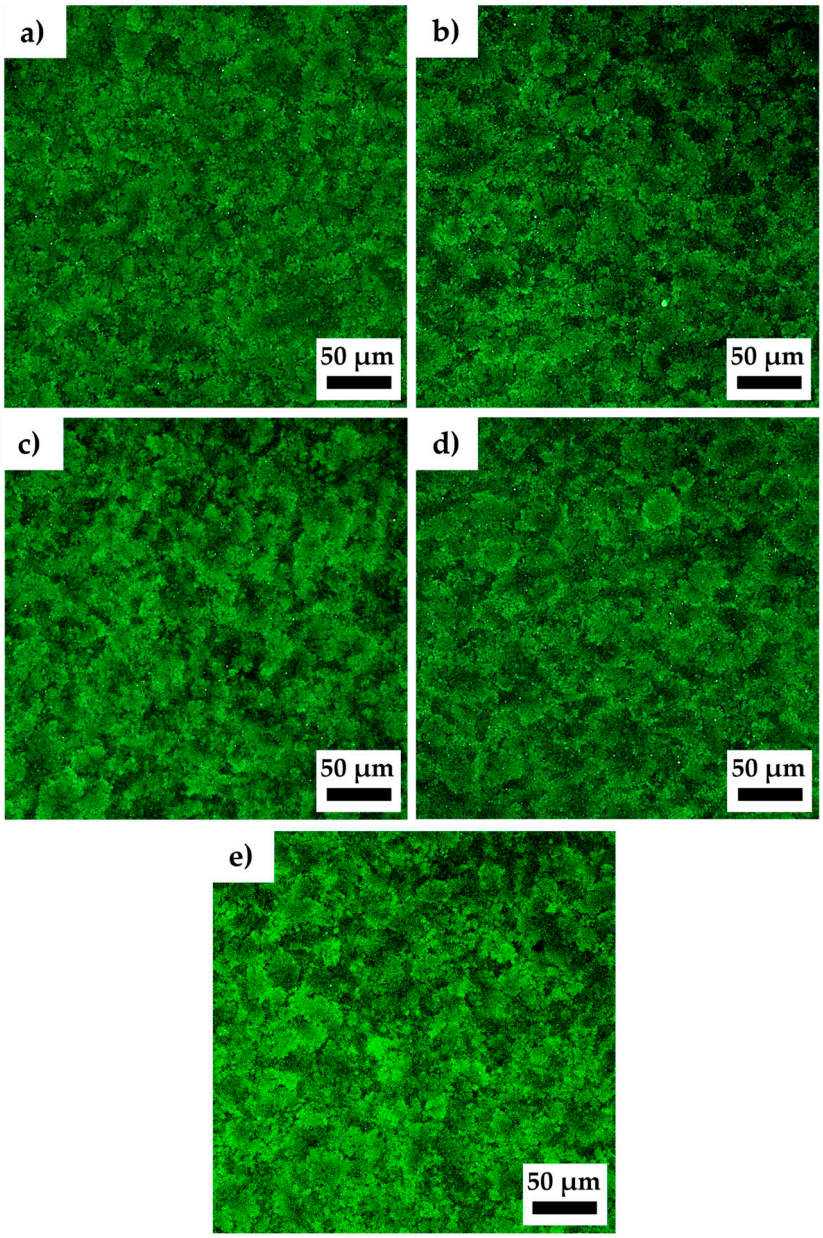

 doi:10.20944/preprints202406.0259.v1

Figure 10. Confocal images of Ultrez 10 microgels with different sonication times (a) SM0, (b) SM60, (c) SM120, (d) SM180, and (e) SDM180.

3. Conclusions

The effect of sonication on the molecular structure of poliacrylic acid (Carbopol® Ultrez 10) and its rheological behavior in aqueous dispersions and microgels containing 0.25 wt. % of the polymer was analyzed in this work by rheometry, molecular weight measurements via static light scattering (SLS), Fourier transform infrared (FTIR) spectroscopy and confocal microscopy. For this, the precursor dispersion and the microgel were sonicated in a commercial ultrasound bath at fixed power and different times. The shear modulus, yield stress and viscosity of the microgel decreased systematically with increasing the sonication time, reflecting a softening of the microgel microstructure. Meanwhile, the overall rheological behavior remained Herschel-Bulkley-like.

SLS measurements evidenced a reduction of the molecular weight of polyacrylic acid with sonication time, this reduced in more than one half after 180 min. FTIR measurements show that sonication produces scission in the C-C links of the Carbopol® backbone, which results in chains with the same chemistry but lower molecular weight. Confocal microscopy measurements revealed a diminution of the size of the microsponge domains with increasing sonication time, which is reflected in a softer microstructure resulting from the reduction of the molecular weight of polyacrylic acid. Finally, the results in this work indicate that both the microstructure and rheological behavior of microgels, in particular, and complex fluids in general, may be manipulated or tailored by high-power ultrasonication.

4. Materials and Methods

The polymer utilized in this work was a poly(acrylic acid), Carbopol® Ultrez 10 (Lubrizol Corporation). Carbopol® resins are hydrophilic cross-linked acrylic acid polymers differing in cross-link density. The more highly cross-linked members of the Carbopol® family are rigid particles, while the more lightly cross-linked members are delivered as micron-sized powder particles, which can swell to a large extent, being these last best representatives of microgels [33]. When the resin is mixed with water, an acid dispersion is obtained. Upon neutralization with a suitable base the protons in the carboxylate groups are substituted by the cation of the base and the molecules adopt a highly expanded configuration. The as-formed highly swollen and deformable particles resemble individual sponges that give rise to elastoviscoplastic microgels [31]. Carbopol® polymers are used in a variety of applications encompassing the cosmetics, pharmaceutical, paint, and food industries as a thickening, suspending, dispersing, and stabilizing agent. In particular, Carbopol® Ultrez 10 is a multi-purpose polymer for a wide range of applications, such as hair gels and skin care emulsion products.

The structure and rheological behavior of Carbopol® dispersions and microgels are dependent on their preparation conditions, including the type of mixing, mixing procedure, and pH [17,34]. Excessive shear during mixing affects the microstructure and rheological behavior of the as formed microgels. Particularly, excessive shear of Carbopol® Ultrez 10 microgels has been reported to produce thixotropy [12]. Therefore, dispersions and microgels in this work were prepared, respectively, following a standard procedure to obtain non-thixotropic or simple yield-stress microgels [11,14,35]. For this, Carbopol® Ultrez 10 was dissolved at 0.25 wt.% in bi-distilled water under continuous stirring at *500 rpm* for *1 h* with a twisted three-blade turbine impeller. Since Carbopol® microgels are sensitive to fungus and bacteria, we added 0.5 wt.% of phenoxyethanol as a preservative to the dispersion to ample its lifetime. Then, the dispersion containing preservative was neutralized with a 5 mol/l NaOH aqueous solution to obtain a pH = 7.02 ± 0.02 while keeping the same stirring conditions until the gel was well formed and free of air bubbles (*0.5 hours*). Once prepared, the microgel sample was maintained at rest in a dark place at ambient temperature for one day. Afterwards, beakers containing *70 ml* of microgel were subjected to sonication for *0*, *60*, *120*, and *180 min*, respectively, in a water-containing ultrasonic cleaner (Cole-Parmer®) of *1.5* liters of capacity and *150 Watts* of sonic power. Sonication started at room temperature (~26°C), which increased up to

 doi:10.20944/preprints202406.0259.v1

63°C after 180 min due to the energy dissipated by the ultrasonic treatment. This temperature rise does not affect the molecular characteristics of Ultrez 10. The samples with different sonication times were labeled as sonicated microgels: SM0, SM60, SM120, and SM180, respectively.

For comparison, another microgel was prepared from a previously sonicated dispersion. In this case, a dispersion containing the same concentration of Ultrez 10 (*0.25 wt%*) was prepared as stated above and left to rest for one day. Afterwards, the dispersion was divided into two parts, and one of these submitted to *180 mins* of sonication. Then the sonicated dispersion was neutralized to obtain another microgel sample labeled as sonicated dispersion microgel: SDM180.

4.1. Rheological Characterization

The rheological behavior of the microgels was assessed *via* small-amplitude oscillatory shear (SAOS) and steady shear measurements using an AR G2 stress-controlled rheometer (TA Instruments) and the parallel-plate geometry. Since this type of microgel is very prone to slip at the shearing surfaces, the plates were covered with sandpaper # 150 to suppress slip [11]. As for the neat dispersions (with and without sonication), their flow behavior was analyzed by using a double-gap Couette cell attached to the AR G2 rheometer. All the flow experiments were performed at 25°C, for this, the rheometer was equipped with Peltier systems for temperature control of both the parallel-plate geometry and double-gap cell. Finally, despite that this microgel preparation procedure resulted in reproducible rheological behavior for up to two weeks [36], all steady and dynamic flow experiments were preceded by a conditioning pre-shear of the microgel at *100* s^{-1} for *60 s*, followed by one minute at rest to eliminate any possible aging affect [37] and to start the rheological experiments with similar gel microstructure [12].

4.2. Determination of Weight-Average Molecular Weight (M_w) of Ultrez 10

To assess possible changes in the molecular characteristics of Carbopol® Ultrez 10 due to sonication, its M_w and the second virial coefficient (A_2) before and after sonication were determined at a temperature of *25°C* by static light scattering (SLS, Litesizer™ 500, Anton Paar GmBH). The SLS technique was chosen because it allows the measurement of absolute M_w [36] and has been successfully used to measure the M_w of other polyelectrolyte molecules [38]. M_w and A_2 are obtained from:

$$\frac{Kc}{R_\theta} = \frac{1}{M_w} + 2A_2c \tag{1}$$

where K is the optical constant, c is the concentration of Carbopol® Ultrez 10 in the solution, and R_θ is the Rayleigh ratio. The K and R_θ were calculated as follows [34]:

$$K = \frac{2\pi^2}{\lambda^4 N_A}\left(n_0 \frac{dn}{dc}\right)^2 \tag{2}$$

$$R_\theta = \frac{(I_s - I_0)n_0^2}{I_T n_T^2} R_T \tag{3}$$

In Equation 2, λ = 658 nm is the wavelength of the incident light, N_A is the Avogadro's number, n_0 = 1.332485 is the refractive index of solvent (bidistilled water), and dn/dc is the rate of change of the refractive index as a function of concentration. In Equation 3, I_S and I_0 are the scattered light intensities of solutions and solvent, respectively, I_T is the dispersed light intensity of a standard (toluene in this case), n_T = 1.48983 is the refractive index of toluene, and $R_T = 1.14574 \times 10^{-5}$ cm^{-1} is the Rayleigh's ratio of toluene.

To measure the molecular weight of the Ultrez 10 before and after sonication, 6 aqueous dissolutions were prepared from the sonicated (SD180) and non-sonicated (SD180) dispersions, both with initial concentration of *2.5* mg/mL. The dissolutions were prepared at 10, 20, 30, 40, 60 and 80%

 doi:10.20944/preprints202406.0259.v1

for which the refractive index as a function of Ultrez 10 concentration was first determined using a refractometer (Abbemat 550, Anton Paar). For the refractive index determination, *0.3* mL of each sample measured with a micropipette were placed in the refractometer. The refractive index of the bidistilled water used to prepare the microgels and dissolution was then found to be n=1.332485 (see Table 2). These data were used to compute the Kc/R_θ values and afterward to determine the molecular weight using the SLS technique. For this, *1.2* mL of each dissolution was added into a clean cuvette of quartz, which was in turn inserted in the Litesizer to start measurements. All experiments were carried out at 25 ºC.

4.3. Confocal Microscopy

The changes in microgel microstructure along with sonication time, were assessed by confocal microscopy using a LSM 800 (ZEISS) microscope with a green light excitation λ=532 nm and the Efficient Navigation Software (Zeiss, version 2.6 Blue edition). For this, a few drops of a $1.1x10^{-4}$ M Rhodamine 6G aqueous solution [12] were added to the samples and gently mixed to obtain uniform red colored microgels. Then, the microgel samples were placed on glass slides for observation. The micrographs were acquired with apochromatic objectives of 20X and 40X with numerical aperture of 0.8 and 1.3, respectively.

4.4. Fourier Transform Infrared Spectroscopy

The identification of the functional groups of the non-sonicated and sonicated lyophilized Ultrez 10 samples was carried out by Fourier transform infrared spectroscopy (FTIR) using a Shimadzu spectrometer (IRAffinity, Japan) with an Attenuated Total Reflection (ATR) accessory in the absorbance mode, and in the wavenumber range from 600 to 3800 cm^{-1}, with 4 cm^{-1} resolution, 16 scans. To obtain the FTIR spectrum of the Carbopol® Ultrez 10 before and after sonication, the dispersions SD0 and SD180 were dried by lyophilization. For this, 100 mL of the dispersion were placed in a lyophilization vessel, frozen at −10 °C, and then introduced into a lyophilizer (LABCONCO FreeZone 6). Freeze drying was carried out for eight hours/day for three days at a vacuum pressure of 7×10^{-3} mBar and a temperature of −25 °C. At the end of each day, the vessel was placed in a freezer to continue the process the next day. Then, 1 mg of the lyophilized Ultrez 10 powders was placed and gently pressed against a high-refractive-index diamond prism located in the ATR accessory to measure the infrared spectrum.

Author Contributions: Conceptualization, J. P-G.; methodology, J. P-G., Y. M-C., F. R-G., E. F. M-B, B. M. M-S.; validation, J. P-G., Y. M-C., F. R-G., E. F. M-B, B. M. M-S.; software, E. F. M-B, B. M. M-S.; formal analysis, J. P-G., F. R-G., E. F. M-B, B. M. M-S.; data curation, Y. M-C., F. R-G., E. F. M-B, B. M. M-S.; writing—original draft preparation, J. P-G.; writing—review and editing, J. P-G., F. R-G., E. F. M-B, B. M. M-S.; visualization, F. R-G., B. M. M-S.; supervision, J. P-G. All authors have read and agreed to the published version of the manuscript.

Funding: This research received no external funding.

Institutional Review Board Statement: Not applicable.

Informed Consent Statement: Not applicable.

Data Availability Statement: The raw/processed data required to reproduce these findings are available upon request.

Acknowledgments: This research was supported by SIP-IPN (Projects Nos. 20230339 and 20241280). E.F.M.-B. is a recipient of a CONAHCYT Postdoctoral Fellowship.

Conflicts of Interest: The authors declare no conflict of interest.

References

1. Lorimer, J. P.; Mason, T. J. Sonochemistry Part 1-The Physical Aspects. *Chem. Soc. Rev.* **1987**, *16*, 239-274. https://doi.org/10.1039/CS9871600239
2. Lindley, J.; Mason, T. J. Sonochemistry Part 2-Synthetic Applications. *Chem. Soc. Rev.* **1987**, *16*, 275-311. https://doi.org/10.1039/CS9871600275

3. Royal Society of Chemistry. Available online: https://www.rsc.org/publishing/journals/prospect/ontology.asp?id=cmo:0001708 (accessed on 13 September 2023)
4. Mason, T. J.; Lorimer, J. P. Applied Sonochemistry, The Uses of Power Ultrasound in Chemistry and Processing, 1st ed.; Wiley-VCH: Weinheim, Germany, 2002; pp. 131–156.
5. Gallo, M.; Ferrara, L.; Naviglio, D. Application of Ultrasound in Food Science and Technology: A Perspective. *Foods* **2018**, 7, 164. doi:10.3390/foods7100164.
6. Bhargava, N.; Mor, R. S.; Kumar, K.; Sharanagat, V. S. Advances in application of ultrasound in food processing: A review. *Ultrason. Sonochem.* **2021**, *70*, 105293. https://doi.org/10.1016/j.ultsonch.2020.105293
7. Chavan, P.; Sharma, P.; Sharma, S. R.; Mittal, T. C.; Jaiswal, A. K. Application of High-Intensity Ultrasound to Improve Food Processing Efficiency: A Review. *Foods* **2022**, *11*, 122. https://doi.org/10.3390/foods11010122
8. Seshadri, R.; Weiss, J.; Hulbert, G. J.; Mount, J. Ultrasonic processing influences rheological and optical properties of high-methoxyl pectin dispersions. *Food Hydrocoll.* **2003**, *17*, 191–197. https://doi.org/10.1016/S0268-005X(02)00051-6
9. Zheng, J.; Zeng, R.; Kan, J.; Zhang, F. Effects of ultrasonic treatment on gel rheological properties and gel formation of high-methoxyl pectin. *J. Food Eng.* **2018**, *231*, 83-90. https://doi.org/10.1016/j.jfoodeng.2018.03.009
10. Gibaud, T.; Dagès, N.; Lidon, P.; Jung, G.; Ahouré, L. C.; Sztucki, M.; Poulesquen, A.; Hengl, N.; Pignon, F.; Manneville, S. Rheoacoustic Gels: Tuning Mechanical and Flow Properties of Colloidal Gels with Ultrasonic Vibrations. *Phys. Rev. X* **2020**, *10*, 011028, https://doi.org/10.1103/PhysRevX.10.011028
11. Medina-Bañuelos, E. F.; Marín-Santibáñez, B. M.; Chaparian, E.; Owens, C. E.; McKinley, G. H.; Pérez-González, J. Rheo-PIV of yield-stress fluids in a 3D-printed fractal vane-in-cup geometry. *J. Rheol*. **2023**, *67*, 891-891. https://doi.org/10.1122/8.0000639
12. Dinkgreve, M.; Fazilati, M.; Denn, M. M.; Bonn, D. Carbopol: From a simple to a thixotropic yield stress fluid. *J. Rheol.* **2018**, *62*, 773-780. https://doi.org/10.1122/1.5016034
13. Medina-Bañuelos, E. F.; Marín-Santibáñez, B. M.; Pérez-González, J. Rheo-PIV study of slip effects on dynamic oscillatory shear measurements of a yield-stress fluid. J. Rheol. **2024**, 68, 361-379. https://doi.org/10.1122/8.0000750
14. Medina-Bañuelos, E. F.; Marín-Santibáñez, B. M.; Pérez-González, J.; Malik, M.; Kalyon, D. M. Tangential annular (Couette) flow of a viscoplastic microgel with wall slip. *J. Rheol.* **2017**, *61*, 1007-1022. https://doi.org/10.1122/1.4998177
15. Gutowski, I. A.; Lee, D.; ·de Bruyn, J. R.; · Frisken, B. J. Scaling and mesostructure of Carbopol dispersions. *Rheol Acta* **2012**, *51*, 441–450. https://doi.org/10.1007/s00397-011-0614-6
16. Medina-Bañuelos, E. F.; Marín-Santibáñez, B. M.; Pérez-González, J. Rheo-PIV analysis of the steady torsional parallel-plate flow of a viscoplastic microgel with wall slip. J. Rheol. **2022**, 66, 31-48. https://doi.org/10.1122/8.0000310
17. Varges, P. R.; Costa, C. M.; Fonseca, B. S.; Naccache, M. F.; de Souza Mendes, P. R. Rheological Characterization of Carbopol® Dispersions in Water and in Water/Glycerol Solutions. *Fluids* **2019**, *4*, 3. https://doi.org/10.3390/fluids4010003
18. Cloitre, M.; Borrega, R.; Monti, F.; Leibler, L. Structure and flow of polyelectrolyte microgels: from suspensions to glasses. *C. R. Physique* **2003**, *4*, 221-230. https://doi.org/10.1016/S1631-0705(03)00046-X
19. Steinman, N. Y.; Bentolila, N. Y.; Domb, A. J. Effect of Molecular Weight on Gelling and Viscoelastic Properties of Poly(caprolactone)–b-Poly(ethylene glycol)–b-Poly(caprolactone) (PCL–PEG–PCL) Hydrogels. *Polymers* **2020**, *12*, 1-11. https://doi.org/10.3390/polym12102372
20. Henglein, A. Chemical effects of continuous and pulsed ultrasound in aqueous solutions. *Ultrason. Sonochem.* **1995**, *2*, S115-S121. https://doi.org/10.1016/1350-4177(95)00022-X
21. Schittenhelm, N.; Kulicke, W.-M. Producing homologous series of molar masses for establishing structure-property relationships with the aid of ultrasonic degradation. *Macromol. Chem. Phys.* **2000**, *201*, 1976–1984. https://doi.org/10.1002/1521-3935(20001001)201:15<1976::AID-MACP1976>3.0.CO;2-0
22. Zhong, K.; Zhang, Q.; Tong, L.; Liu, L.; Zhou, X.; Zhou, S. Molecular weight degradation and rheological properties of schizophyllan under ultrasonic treatment. *Ultrason. Sonochem.* **2015**, *23*, 75–80. http://dx.doi.org/10.1016/j.ultsonch.2014.09.008
23. Teraoka, I. Polymer solutions: An introduction to physical properties. John Wiley & Sons Inc. (Chapter 1) **2002**.
24. Grönroos, A.; Pirkonen, P.; Heikkinen, J.; Ihalainen, J.; Mursunen, H.; Sekki, H. Ultrasonic depolymerization of aqueous polyvinyl alcohol. *Ultrason. Sonochem.* **2001**, *8*, 259–264. https://doi.org/10.1016/S1350-4177(01)00086-4
25. Rokita, B.; Czechowska-Biskup, R.; Ulanski, P.; Rosiak, J. M. Modification of polymers by ultrasound treatment in aqueous solution. *e-Polymers* **2005**, *024*, 1-12. https://doi.org/10.1515/epoly.2005.5.1.261

 doi:10.20944/preprints202406.0259.v1

26. Mohod, A. V.; Gogate, P. R. Ultrasonic degradation of polymers: Effect of operating parameters and intensification using additives for carboxymethyl cellulose (CMC) and polyvinyl alcohol (PVA). *Ultrason. Sonochem.* **2011**, *18*, 727-734. https://doi.org/10.1016/j.ultsonch.2010.11.002
27. Venegas-Sanchez, J. A.; Tagaya, M.; Kobayashi, T. Effect of ultrasound on the aqueous viscosity of several water-soluble polymers. *Polym. J.* **2013**, *45*, 1224-1233. https://doi.org/10.1038/pj.2013.47
28. Prajapat, A. L.; Gogate, P. R. Intensification of degradation of guar gum: Comparison of approaches based on ozone, ultraviolet and ultrasonic irradiations. *Chem. Eng. Process.* **2015**, *98*, 165–173. https://doi.org/10.1016/j.cep.2015.09.018
29. Prajapat, A. L.; Gogate, P. R. Intensification of depolymerization of polyacrylic acid solution using different approaches based on ultrasound and solar irradiation with intensification studies. *Ultrason. Sonochem.* **2016**, *32*, 290-299. https://doi.org/10.1016/j.ultsonch.2016.03.022
30. Feng, L.; Cao, Y.; Xu, D.; Wang, S.; Zhang, J. Molecular weight distribution, rheological property and structural changes of sodium alginate induced by ultrasound. *Ultrason. Sonochem*. **2017**, *34*, 609–615. https://doi.org/10.1016/j.ultsonch.2016.06.038
31. Piau, J. M. Carbopol gels: Elastoviscoplastic and slippery glasses made of individual swollen sponges: Meso- and macroscopic properties, constitutive equations and scaling laws. *J. Non-Newtonian Fluid Mech.* **2007**, *144*, 1-29. https://doi.org/10.1016/j.jnnfm.2007.02.011
32. Oelschlaeger, C.; Marten, J.; Péridont, F.; Willenbacher, N. Imaging of the microstructure of Carbopol dispersions and correlation with their macroelasticity: A micro- and macrorheological study. *J. Rheol.* **2022**, *66*, 749–760. https://doi.org/10.1122/8.0000452
33. Carnal, J. O.; Naser, M. S. The use of dilute solution viscometry to characterize the network properties of Carbopol microgels. *Colloid. Polym. Sci.* **1992**, *270*, 183-193. https://doi.org/10.1007/BF00652185
34. Baudonnet, L.; Grossiord, J. L.; Rodriguez, R. Effect of dispersion stirring speed on the particle size distribution and rheological properties of three carbomers. *J. Disper. Sci. Technol.* **2004**, *25*, 183–192. https://doi.org/10.1081/DIS-120030665
35. Medina-Bañuelos, E. F.; Marín-Santibáñez, B. M.; Pérez-González, J. Rheo-PIV analysis of the vane in cup flow of a viscoplastic microgel. *J. Rheol*. **2019**, *63*, 905-915. https://doi.org/10.1122/8.0000310
36. Sperling, L. H. (2001). *Introduction to physical polymer science*. John Wiley & Sons Inc. (Chapter 3).
37. Agarwal, M.; Joshi, Y. M. Signatures of physical aging and thixotropy in aqueous dispersion of Carbopol. Phys. Fluids **2019**, 31, 063107. https://doi.org/10.1063/1.5097779
38. Rodríguez-González, F.; Pérez-González, J.; Muñoz-López, C. N.; Vargas-Solano, S. V.; Marín-Santibáñez, B. M. Influence of age on molecular characteristics and rheological behavior of nopal mucilage. *Food Sci. Nutr.* **2021**, *9*, 6776-6785. https://doi.org/10.1002/fsn3.2629